

Title	A hybrid TOA and RSS-based factor graph for wireless geolocation technique
Author(s)	Karimah, Shofiyati Nur; Aziz, Muhammad Reza Kahar; Matsumoto, Tad
Citation	2016 IEEE 12th International Colloquium on Signal Processing & Its Applications (CSPA): 140-145
Issue Date	2016
Type	Conference Paper
Text version	author
URL	http://hdl.handle.net/10119/14210
Rights	This is the author's version of the work. Copyright (C) 2016 IEEE. 2016 IEEE 12th International Colloquium on Signal Processing & Its Applications (CSPA), 2016, 140-145. Personal use of this material is permitted. Permission from IEEE must be obtained for all other uses, in any current or future media, including reprinting/republishing this material for advertising or promotional purposes, creating new collective works, for resale or redistribution to servers or lists, or reuse of any copyrighted component of this work in other works.
Description	

A Hybrid TOA and RSS-based Factor Graph for Wireless Geolocation Technique

Shofiyati Nur Karimah¹, Muhammad Reza Kahar Aziz^{1,2}, and Tad Matsumoto^{1,3}

¹Japan Advanced Institute of Science and Technology (JAIST), 1-1 Asahidai, Nomi, Ishikawa, 923-1292 JAPAN

²Electrical Engineering Department, Institute Teknologi Sumatera (ITERA), Lampung Selatan, 35365 INDONESIA

³Centre for Wireless Communications, University of Oulu, Oulu, 90014 FINLAND

Email:{karimah, reza.kahar, matumoto}@jaist.ac.jp

Abstract—This paper proposes a new hybrid time-of-arrival (TOA) and received-signal-strength (RSS)-based factor graph (TRFG) for wireless geolocation technique. The TOA-based FG (TFG) provides rough estimated position which is used to select the most appropriate monitoring spot positions, i.e., at least four monitoring spots surrounding the target, and initial target position for RSS-based FG (RFG) technique. The performance of the proposed technique is verified through making comparison with the conventional TFG-only technique suffering from imperfect time synchronization, as well as with the idealistic RFG technique, in terms of the root mean squared error (RMSE) of the estimate. It is shown that the RFG technique utilizing the result of TFG achieves close performance to the idealistic RFG technique where the optimal monitoring spots are assumed to be always correctly identified. Hence, the proposed technique outperforms the TFG-only technique in terms of estimation accuracy.

Index Terms—factor graph, TOA, RSS, wireless geolocation, sensor network

I. INTRODUCTION

High accuracy wireless geolocation techniques have become an important issue in the past two decades due to the increasing demand for recent and future location based wireless systems. This technology is of crucial significance for many location-based service applications, such as Emergency-911 (E-911), location-sensitive billing, and smart transportation systems [1]–[3]. Some geometry-based measurements for wireless geolocation techniques have been proposed, including time-of-arrival (TOA), angle-of-arrival (AOA), received-signal-strength (RSS), and time-difference-of-arrival (TDOA) [4]. In 2003, a technique utilizing stochastic properties of the measurements was proposed to perform location detection using factor graph (FG) introduced by [5]. The sum-product algorithm, used for efficiently calculating the probability marginals, using the mathematical framework of the FG was first introduced in [6]. Hence, the FG can effectively coordinate all stochastic information to obtain high accuracy in geolocation. Only mean and variance are used, in the FG, with the Gaussianity assumption of the measurement error. In addition, in the FG, the global function is decomposed into several local functions resulting the reduction of computational complexity [6], [7].

This paper proposes a new hybrid TOA and RSS based factor graph (TRFG) technique for wireless geolocation, where

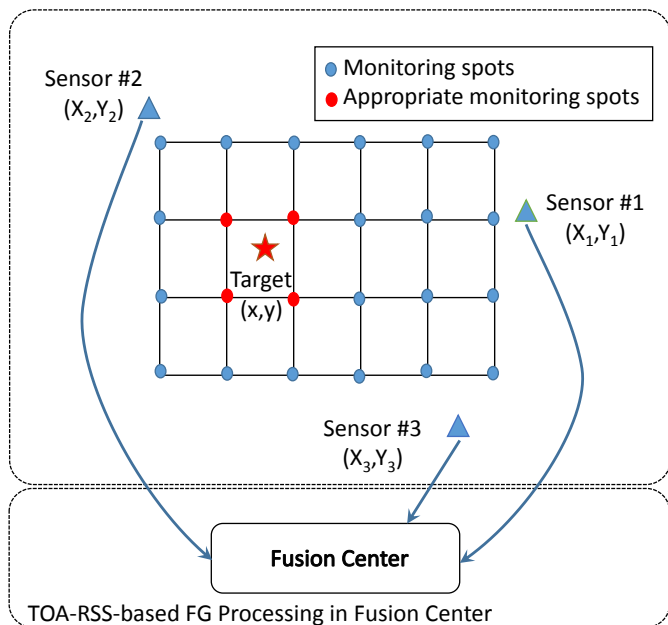


Fig. 1. A basic structure of TRFG wireless geolocation technique depicts the sensors, target, monitoring spots, appropriate monitoring spots, and fusion center.

the TFG is used to provide rough estimated position for selecting the appropriate monitoring spots surrounding the target. The selected monitoring spots are then used by the RFG technique in scenario shown in Fig. 1 to estimate the location of the target. The RFG, introduced in [8], uses pattern recognition, i.e., RADAR¹ algorithm [11], to select the four appropriate monitoring spots surrounding the target. However, the monitoring spots selection is not enough precisely described in [8]. The TFG technique, which is introduced in [5], needs perfect timing synchronism, however, it is difficult in practical implementations. Therefore, those two techniques are combined, where TFG is used for providing the rough estimated position used as initial point and to select the appropriate monitoring spots, by which the timing synchronism

¹RADAR: a radio-frequency (RF) based system for locating and tracking users inside buildings

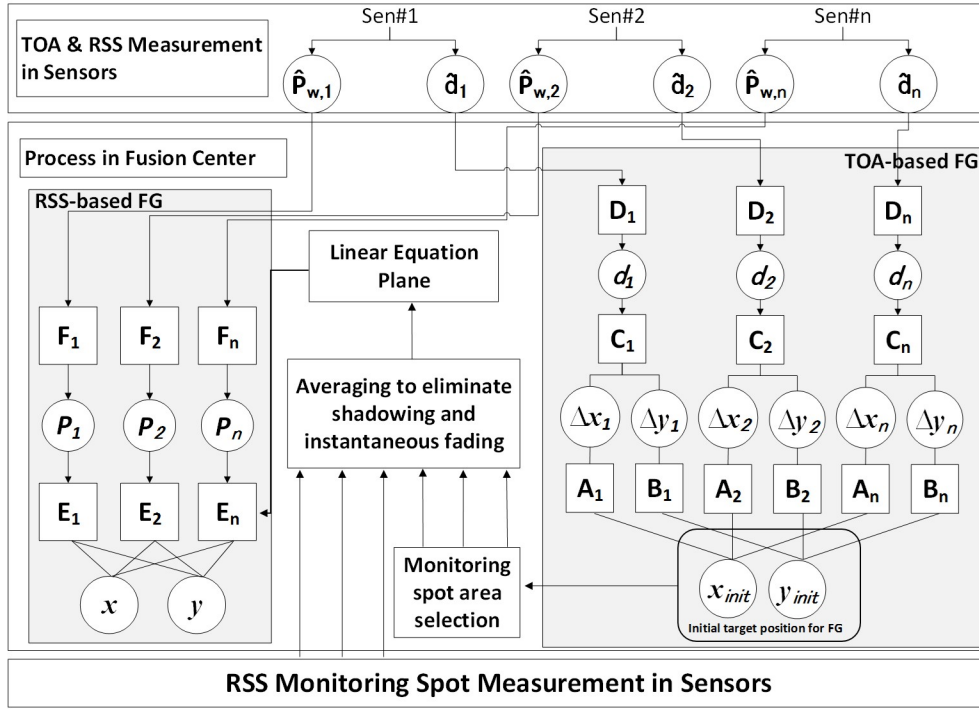


Fig. 2. The proposed TRFG for wireless geolocation.

sensitivity problem can well be avoided, while RFG utilizes the selected monitoring spots for detailed detection. The proposed technique is referred to as hybrid TOA-RSS-based FG (TRFG) technique. It is shown that the proposed TRFG technique can achieve equivalent performance to the idealistic RFG which assumes that the optimal monitoring spots are always selected.

This paper is organized as follows. Section II describes the system model of the proposed technique depicted in Fig. 2 and detail the RSS-based and TOA-based FG algorithms in the figure. The results of the simulations conducted to evaluate the performance of the proposed algorithm are given in Section III. Section IV concludes this paper.

II. SYSTEM MODEL

The range and received signal power measurements are used to estimate the position of the target. In the proposed technique, each of the sensors, of which positions are known to the fusion center, send both information of time of arrival which has been converted to distance \hat{d} and received signal power in watts \hat{P}_w . \hat{d} and \hat{P}_w are obtained through the training process conducted beforehand, and used as reference information in the TFG and RFG techniques, respectively, in the target detection process. As in the standard TOA-based positioning technique, the range measurements provided by, at least, $n = 3$ sensors are available. Then, 2-dimensional (X, Y) estimated position can be performed.

The TFG used in this paper is based on the technique introduced in [7], where account is taken of the imperfect time synchronism because as noted in [7] that $1 \mu s$ synchronization inaccuracy, for example, leads to 300 meters estimation

error due to the very high velocity of electromagnetic wave propagation, 3×10^8 meter/second. The imperfect timing synchronization as well as multipath effect due to non-line-of-sight (NLOS) signal components are included as measurement error. The measurement error is assumed as being equivalent to non-zero Gaussian noise. This assumption is reasonable because the accumulated effect of many independent factors results in Gaussian distributed measurement, as mentioned in [7], [8]. The result of the TFG based algorithm are used for selecting the monitoring spots, and also as the initial point for the RFG technique. Besides the technique presented in this paper, an alternative technique for identifying the appropriate monitoring spots is proposed in [10] where a voronoi graph is utilized. However, making performance comparison with the technique shown in [10] is out of the scope of this paper.

Basically, the RFG technique is based on [8]. However, the scenario assumption of indoor [8] is modified to outdoor environments in this paper, shadowing and instantaneous fading variations are eliminated by performing much averaging the RSS measurement around the enough wide vicinity of the monitoring spots in the training process. Hence, there only path-loss remains in the input data to the RFG algorithms.

A. ToA-based Geolocation Technique

In this sub-section, the TFG algorithm is briefly described, of which details are introduced in [7]:

Step-1 Assuming that all sensors are synchronized. Each sensor converts the measured noise-corrupted TOA into the distance information \hat{d} . Let the measured distance data set be denoted by \hat{d}_i , which is transmitted to the fusion center.

As stated before, the measurement data distributes over a Gaussian distribution as a result of a lot of imperfections. The node D_i in the TFG calculates the mean and variance of the data \hat{d}_i sent from the i -th sensor, $i = 1, 2, \dots, n$. The calculated mean m_i and variance σ_i^2 are used in the probability density function (pdf) of \hat{d}_i , as

$$\mathcal{N}(\hat{d}_i, m_i, \sigma_i^2) \propto \exp\left[-\frac{(\hat{d}_i - m_i)^2}{2\sigma_i^2}\right]. \quad (1)$$

The calculated m_i and σ_i^2 are sent through the passing node d_i as shown in Fig. 2, as the soft information (SI) to be exchanged in the factor graph.

Step-2 Variable node d_i passes the generated SI, in the form of mean $m_{d_i \rightarrow C_i}$ and variance $\sigma_{d_i \rightarrow C_i}^2$ of the distance d_i , from factor node D_i to factor node C_i .

Step-3 Factor node C_i converts the distance \hat{d}_i information into the x-coordinate and y-coordinate, according to the Pythagorean law.

$$(d_i^k)^2 = (\Delta x_i^k)^2 + (\Delta y_i^k)^2, \quad (2)$$

where k is iteration index. Therefore the mean and variance calculated in factor node C_i are expressed as

$$\begin{aligned} m_{C_i \rightarrow \Delta x_i} &= \pm \sqrt{m_{d_i \rightarrow C_i}^2 - m_{\Delta x_i \rightarrow C_i}^2}, \\ m_{C_i \rightarrow \Delta y_i} &= \pm \sqrt{m_{d_i \rightarrow C_i}^2 - m_{\Delta y_i \rightarrow C_i}^2}, \end{aligned} \quad (3)$$

$$\begin{aligned} \sigma_{C_i \rightarrow \Delta x_i}^2 &= \frac{m_{\Delta y_i \rightarrow C_i}^2 \sigma_{\Delta y_i \rightarrow C_i}^2 + m_{d_i \rightarrow C_i}^2 \sigma_{d_i \rightarrow C_i}^2}{m_{d_i \rightarrow C_i}^2 - m_{\Delta y_i \rightarrow C_i}^2}, \\ \sigma_{C_i \rightarrow \Delta y_i}^2 &= \frac{m_{\Delta x_i \rightarrow C_i}^2 \sigma_{\Delta x_i \rightarrow C_i}^2 + m_{d_i \rightarrow C_i}^2 \sigma_{d_i \rightarrow C_i}^2}{m_{d_i \rightarrow C_i}^2 - m_{\Delta x_i \rightarrow C_i}^2}. \end{aligned} \quad (4)$$

Step-4 Then relative variable nodes Δx_i and Δy_i forward the message back and forth between factor node C_i and both factor node A_i and B_i , as

$$m_{\Delta x_i \rightarrow C_i} = m_{A_i \rightarrow \Delta x_i}, \quad (5)$$

$$m_{\Delta y_i \rightarrow C_i} = m_{B_i \rightarrow \Delta y_i},$$

$$\sigma_{\Delta x_i \rightarrow C_i}^2 = \sigma_{A_i \rightarrow \Delta x_i}^2, \quad (6)$$

$$\sigma_{\Delta y_i \rightarrow C_i}^2 = \sigma_{B_i \rightarrow \Delta y_i}^2,$$

$$m_{\Delta x_i \rightarrow A_i} = m_{C_i \rightarrow \Delta x_i}, \quad (7)$$

$$m_{\Delta y_i \rightarrow B_i} = m_{C_i \rightarrow \Delta y_i},$$

$$\sigma_{\Delta x_i \rightarrow A_i}^2 = \sigma_{C_i \rightarrow \Delta x_i}^2, \quad (8)$$

$$\sigma_{\Delta y_i \rightarrow B_i}^2 = \sigma_{C_i \rightarrow \Delta y_i}^2.$$

Step-5 Factor nodes A_i and B_i convert relative location information into the absolute location information which is calculated in the variable nodes x_{init} and y_{init} . It should be noted that the location (X_i, Y_i) of sensors have been already known. The SI which is calculated in the nodes A_i and B_i are described as

$$m_{A_i \rightarrow x_i} = X_i - m_{\Delta x_i \rightarrow A_i}, \quad (9)$$

$$m_{B_i \rightarrow y_i} = Y_i - m_{\Delta y_i \rightarrow B_i},$$

$$\sigma_{A_i \rightarrow x_i}^2 = \sigma_{\Delta x_i \rightarrow A_i}^2, \quad (10)$$

$$\sigma_{B_i \rightarrow y_i}^2 = \sigma_{\Delta y_i \rightarrow B_i}^2,$$

$$m_{A_i \rightarrow \Delta x_i} = X_i - m_{x_i \rightarrow A_i}, \quad (11)$$

$$m_{B_i \rightarrow \Delta y_i} = Y_i - m_{y_i \rightarrow B_i},$$

$$\sigma_{A_i \rightarrow \Delta x_i}^2 = \sigma_{x_i \rightarrow A_i}^2, \quad (12)$$

$$\sigma_{B_i \rightarrow \Delta y_i}^2 = \sigma_{y_i \rightarrow B_i}^2,$$

where (9) and (10) are mean and variance from factor node A_i and B_i to variable node x_{init} and y_{init} , while (11) and (12) are mean and variance to be forwarded from factor node A_i and B_i to variable node Δx_i and Δy_i .

Step-6 When the messages reach variable nodes x_{init} and y_{init} , all the messages from factor nodes A_i are summed in variable node x_{init} , and the messages from factor nodes B_i are summed by the variable node y_{init} , according to the sum-product algorithm. Equation (13) described below shows the general notation of the sum-product algorithm in the pdf domain which is used in factor graph [6]–[8].

$$\prod_{j=1, j \neq i}^N \mathcal{N}(x, m_j, \sigma_j^2) \propto \mathcal{N}(x, m_\Lambda, \sigma_\Lambda^2) \quad ; j = 1, 2, \dots, N, \quad (13)$$

with j being the sensor index. Equation (13) uses the fact that product of independent identically distributed (i.i.d) Gaussian variables are still Gaussian distributed [10]. Referring to [6], a close form of the sum-product algorithm which is proposed run in variable node x_{init} , and the result to be forwarded back to factor node A is expressed as

$$\frac{1}{\sigma_{x_{init} \rightarrow A_i}^2} = \sum_{j=1, j \neq i}^N \frac{1}{\sigma_{A_j \rightarrow x}^2}, \quad (14)$$

$$m_{x_{init} \rightarrow A_i} = \sigma_{x_{init} \rightarrow A_j}^2 \sum_{j=1, j \neq i}^N \frac{m_{A_j \rightarrow x}}{\sigma_{A_j \rightarrow x}^2}. \quad (15)$$

The procedure (14) and (15) for variable node x_{init} above can be applied similarly to variable node y_{init} .

Step-7 Repeat the process of step 3) to 6).

Step-8 After the iteration converges, the variable nodes x_{init} and y_{init} combine all incoming information from all factor nodes A_i and B_i by modifying the index of the messages given by (14) and (15), as

$$\frac{1}{\sigma_{x_{init}}^2} = \sum_{i=1}^N \frac{1}{\sigma_{A_i \rightarrow x}^2}, \quad (16)$$

$$m_{x_{init}} = \sigma_{x_{init} \rightarrow A_i}^2 \sum_{i=1}^N \frac{m_{A_i \rightarrow x}}{\sigma_{A_i \rightarrow x}^2}. \quad (17)$$

The calculation of equations (16) and (17) are also proposed to obtain $m_{y_{init}}$. Those mean value vectors $(m_{x_{init}}, m_{y_{init}})$

²The arrows \rightarrow denotes the message flow between the nodes.

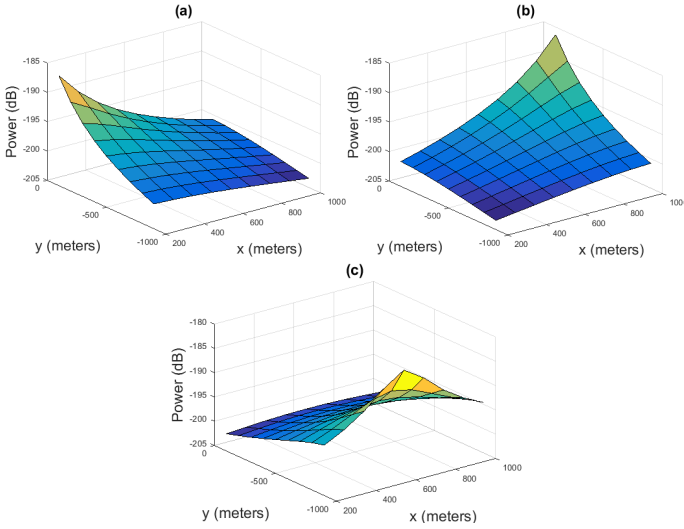


Fig. 3. (a) Pathloss profile of sensor 1=(100,0), (b) Pathloss profile of sensor 2=(1100,0), (c) Pathloss profile of sensor 3=(600,-1000)

indicate the rough estimation of TOA which is used for selecting four monitoring spots as has been done in [10]. The rough estimation of TOA is also used as initial point in the RFG. If the selected monitoring spots are the closest cover to the real target, they are called "idealistic" ones.

B. RSS-based Geolocation Technique

The first process in the RFG technique is to provide graph with RSS measurement in watts ($\hat{P}_{w,i}$) from sensors as the SI as mentioned, before, RSS containing the path-loss information only is processed in the fusion center. Hence, the RSS path-loss exponent model shown as following equations.

$$PLF = 20 \log_{10} \left(\frac{4\pi d_0 f}{c} \right), \quad (18)$$

$$PLE(d) = -PLF - 10n_p \log_{10} \left(\frac{d}{d_0} \right), \quad (19)$$

where PLF and PLE , both in dB, are free space path-loss and path-loss exponent measurement, respectively. d , d_0 , f , c , and n_p are euclidean distance in meter, reference distance of path-loss exponential model in meter, carrier frequency in hertz, velocity of light in m/s, and coefficient of path-loss exponent, respectively. Fig. 3 depicts the RSS profile of each sensors suffering pathloss only.

The RFG algorithm is briefly described, in which the detail can be found in [8]. The sample of measurement, obtained by the factor node F , is corrupted by zero mean Gaussian. The variable node P passes the logarithmic scale of RSS in dB to the linear plane least square (LS) in the factor node E as the SI message. Factor node E converts the RSS SI of the target to be the target coordinate SI by using the linear plane

equation.³ The linear plane equation created in factor node E has been derived in [8], as

$$a_x \cdot x + a_y \cdot y + a_p \cdot p = c, \quad (20)$$

where a_x , a_y , and a_p are coefficients of the plane equation; x and y are axes 2-D linear scale plane which is represented as monitoring spots grid; p is the RSS at the node (x, y) appropriated by the linear plane in the logarithmic scale; and c is non-zero constant which is set to one in this paper.

The LS algorithm is used to obtain the coefficients a_x , a_y , and a_p . Equation (20) can be expressed into matrix as

$$\mathbf{B} \cdot \mathbf{a} = \mathbf{C}, \quad (21)$$

where \mathbf{B} is matrix of x , y , and p ; and \mathbf{a} is vector of coefficients. The LS solution to (20) is the given by

$$\mathbf{a} = (\mathbf{B}^T \cdot \mathbf{B})^{-1} \cdot \mathbf{B}^T \cdot \mathbf{C}. \quad (22)$$

The linear planes created in factor node E are shown in Fig. 4. When the coefficients in \mathbf{a} are obtained, the mean and variance of RSS can be obtained by the following expression [10]

$$m_{E_i \rightarrow x} = \alpha_{x_i} + \beta_{x_i} \cdot m_{y \rightarrow E_i} + \gamma_{x_i} \cdot m_{P_i \rightarrow E_i}, \quad (23)$$

$$\sigma_{E_i \rightarrow x}^2 = \beta_{x_i}^2 \cdot \sigma_{y \rightarrow E_i}^2 + \gamma_{x_i}^2 \cdot \sigma_{P_i \rightarrow E_i}^2. \quad (24)$$

The mean and variance of y ($m_{E_i \rightarrow y}$, $\sigma_{E_i \rightarrow y}^2$), can be obtained in the same way as (23) and (24), as

$$\begin{aligned} \alpha_{x_i} &= c/a_{x_i}, & \alpha_{y_i} &= c/a_{y_i}, \\ \beta_{x_i} &= -a_{y_i}/a_{x_i}, & \beta_{y_i} &= -a_{x_i}/a_{y_i}, \\ \gamma_{x_i} &= -a_{P_i}/a_{x_i}, & \gamma_{y_i} &= -a_{P_i}/a_{y_i}, \end{aligned} \quad (25)$$

After that, the SI are exchanged iteratively between the factor node E and the node (x, y) where sum-product algorithm (13) is used to update the mean and variance of the target coordinates during the iteration until it converges.

III. SIMULATION RESULT

The computer simulations are following the methodology shown in [9] which is conducted to verify the performance of the proposed technique. One round of simulation consist of 1,000 trials. Three sensors used in both the TFG and RFG techniques were fixed at the position (100,0), (1100,0), (600,-1000), as shown in Fig. 5. The standard deviation is set at 300 meters in the TFG simulation.

The monitoring spots position were set in square area, 1,000 x 1,000 m² where the resolution grid at 100 x 100 m². The TFG technique is used to select one cell composed up four monitoring spots which are surrounding the target position. The result is followed by the RFG technique to obtain the accurate estimated location by using those four selected monitoring spots and initial value provided as the result of the TFG.

The RSS value measured at the sensors, in this computer simulation, were obtained from exponential path-loss model

³The equation is created by performing LS to the RSS of training signal and the coordinates of the monitoring spots during off-line phase.

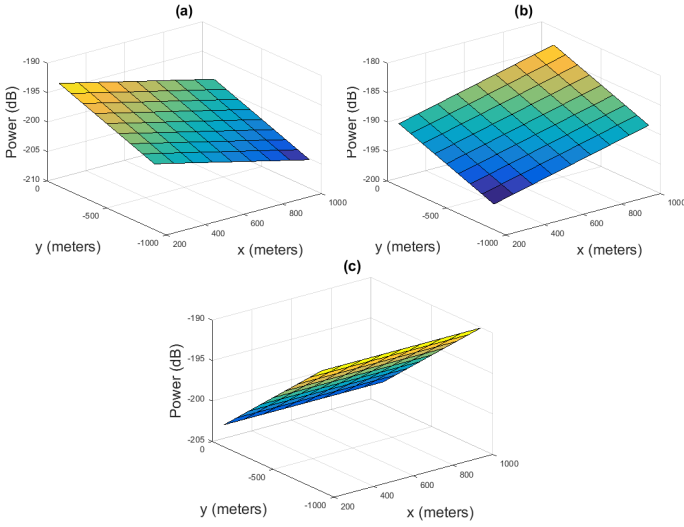


Fig. 4. (a) Linear plane between selected monitoring spots and sensor 1 = (100, 0), (b) Linear plane between selected monitoring spots and sensor 2 = (1100, 0), (c) Linear plane between selected monitoring spots and sensor 3 = (600, -1000)

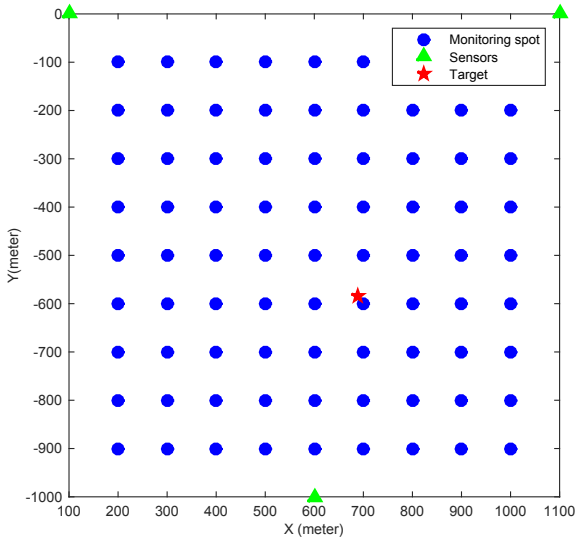


Fig. 5. The simulation scenario depicts the monitoring spots with configuration of grid $4100 \times 100 \text{ m}^2$, three sensors, and 1 target in total area $1,000 \times 1,000 \text{ m}^2$.

with the path-loss exponent $n_p = 3$, reference distance $d_0 = 100 \text{ m}$, and frequency carrier $f = 1e9 \text{ Hz}$.

The following parameters were used to evaluate the proposed technique: a) 50, 100, and 200 iterations for each trial, b) 1000 samples, c) 3 sensors, d) The measurement error values in signal-to-noise ratio (SNR), 0 – 30 dB. In this simulation, assume that the measurement samples are corrupted by measurement error having the same variance in every sensor for simplicity.

Figs. 6 and 7 show trajectory of the proposed technique within the three sensors. Initial point provided by the TRFG

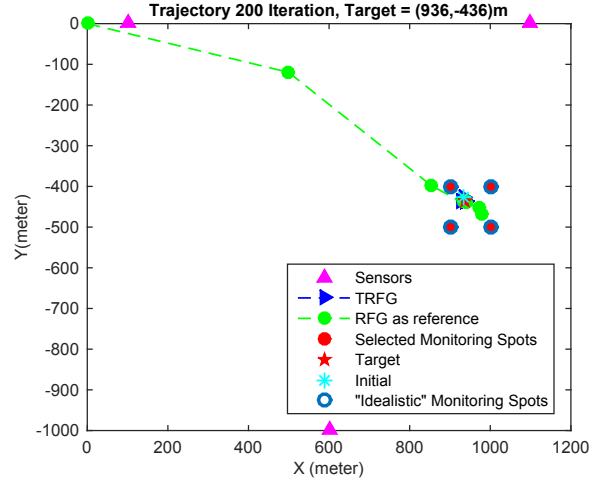


Fig. 6. The trajectory of the TRFG technique with configuration of three sensors and target position at (936, -436) m. The selected monitoring spots are shown in the same position of the proper monitoring spots.

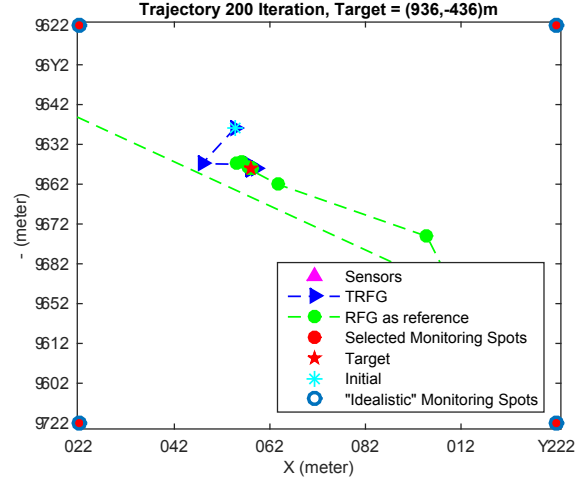


Fig. 7. Zoom of trajectory of the TRFG technique with configuration of three sensors and target position at (936, -436) m. The selected monitoring spots are shown in the same position of the proper monitoring spots.

technique is close to the target position at (936, -436) m. It is found that the selected monitoring spots calculated by the TRFG algorithm are always "idealistic ones", in this series of simulations.

Fig. 8 shows the accuracy of the proposed technique in term of root mean squared error (RMSE) versus SNR. It shows that accuracy of the proposed technique outperforms the TRFG-only technique. The performance of proposed technique is close to the RFG having idealistic monitoring spots. The accuracy is approximately within 1.5 m at 15 dB of SNR .

IV. CONCLUSION

A new wireless geolocation technique using hybrid TOA and RSS factor graph (TRFG) has been proposed in this paper. The TRFG is used for selecting the most appropriate

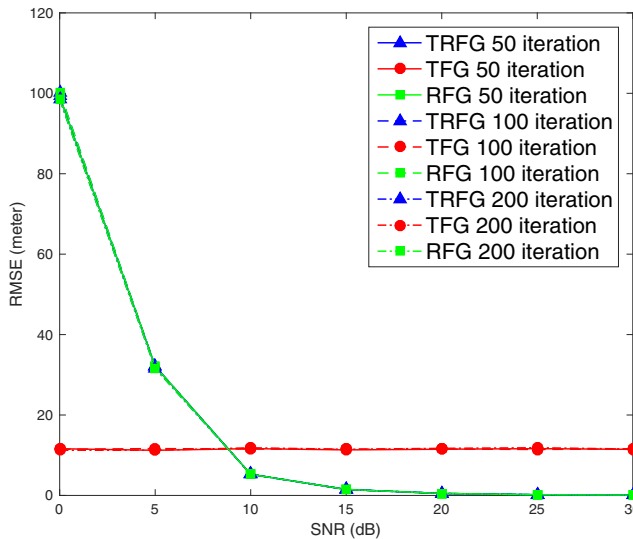


Fig. 8. RMSE of the proposed technique and TFG

four monitoring spots to be utilized in the RFG algorithm. Simulation results show that the proposed technique provides much higher accuracy over the TFG-only in the terms of RMSE. This is because the TFG technique is used only for appropriate monitoring spots identification, by which the problem due to the high sensitivity to timing asynchronism with TFG can well be avoided. It has been shown that RMSE performance of the RFG technique with idealistic monitoring spot selection and the proposed TRFG technique are almost identical, even in the presence of timing asynchronism. This indicates that with the help of the TFG technique, monitoring spots can be selected most suitably for the RFG technique, and hence the performance is equivalent to that with idealistic RFG.

ACKNOWLEDGMENT

This research is in part supported by Koden Electronics Co., Ltd. Authors are very much thankful for their support.

REFERENCES

[1] J. James, J. Caffery and G. L. Stuber, "Overview of radiolocation in CDMA cellular system," *IEEE Communication Magazine*, vol. 36, no. 4, pp. 38-45, April 1998.

[2] K. Pahlavan, X. Li and J. P. Makela, "Indoor geolocation science and technology," *IEEE Communication Magazine*, vol. 40, pp. 112-118, February 2002.

[3] Y. Zhao, "Standardization of mobile phone positioning for 3G system," *IEEE Communication Magazine*, vol. 40, pp. 108-116, July 2002.

[4] J.Figueiras, S.Frattasi, "Mobile Positioning and Tracking From Conventional to Cooperative Techniques," John Wiley Sons Ltd, 2010.

[5] J.-C. Chen, C.-S. Maa, and J.-T. Chen, "Factor graph for mobile position location," *IEEE International Conference on Acoustics, Speech, and Signal Processing (ICASSP) 2003*, vol. 2, pp. 393-396, April 2003.

[6] F. R. Kschischang, B. J. Frey, and H.-A. Loeliger, "Factor graphs and the sum-product algorithm," *IEEE Trans. on Information Theory*, vol. 47, no. 2, pp. 498-519, February 2001.

[7] J.-C. Chen, Y.-C. Wang, C.-S. Maa, and J.-T. Chen "Network side mobile position location using factor graphs," *IEEE Trans. on Wireless Comm.*, vol. 5, no.10, pp. 2696-2704, October 2006.

[8] C.-T. Huang, C.-H. Wu, Y.-N. Lee and J.-T. Chen, "A novel indoor RSS-based position location algorithm using faactor graphs," *IEEE Trans. on Wireless Comm.*, vol. 8, no. 6, pp. 3050-3058, June 2009.

[9] M. R. K. Aziz, Y. Lim, and T. Matsumoto, "A New Wireless Geolocation Technique Using Joint RSS-based Voronoi and Factor Graph," *IEEE Computer Society on Conference: Asia Modelling Symposium (AMS) 2015*, pp. 131-136, September 2015.

[10] M. R. K. Aziz, Y. Lim, and T. Matsumoto, "A New RSS-based Wireless Geolocation Technique Utilizing Joint Voronoi and Factor Graph," *International Journal of Simulation Systems, Science & Technology (IJSSST)*, submitted 30 Nov 2015 (under review).

[11] P. Bahl and V. N. Padmanabhan, "RADAR: an in-building RF-based user location and tracking system," in *Proc. IEEE INFOCOM 2000*, vol. 2, Mar. 2000, pp. 775-784.